

5G MIMO Antenna System Based on Patched Folded Antenna with EBG Substrate

Alaa M. Hediya^{1, *}, Ahmed M. Attiya², and Walid S. El-Deeb³

Abstract—A novel EBG structure in the form of a square spiral cell with a via at its middle is presented in this work to improve the isolation between the antenna elements and also enhance the overall parameters of the proposed MIMO system. Wide BW is achieved for the 6-elements MIMO system operating in the frequency range from 3 GHz to 5 GHz which is suitable for 5G mobile applications. The single antenna element consists of four coupled sections printed on an FR4 substrate. To improve the performance and maintain the BW, the EBG structure is employed to increase the isolation between the antenna elements. The proposed EBG is designed to have a bandgap from 2.5 GHz to 6.5 GHz. The addition of the EBG structure between the radiating elements reduces the envelope correlation coefficient across the whole operating BW. SAR calculations are also performed using head and hand models. The performance of the proposed EBG loaded MIMO antenna is suitable to be a potential competitor for future 5G applications.

1. INTRODUCTION

The fifth-generation (5G) wireless systems have a fantastic impact on social and economic improvement. The 5G networks have sub-six GHz bands of the New Radio (NR) system. Three main bands are used in sub-six GHz 5G applications; N77 (3.3–4.2 GHz), N78 (3.3–3.8 GHz), and N79 (4.4–5.0 GHz). Each country can choose its operating frequency range from these three 5G NR bands. China has used 3.3–3.6 GHz and 4.8–5.0 GHz bands as its specific band to 5G communications, while European Union (EU) has used the 3.4–3.8 GHz band [1–3].

The prerequisite for working in 5G networks is the ability to provide a multi-gigabit per second data rate. This is done by using a multi-input-multi-output (MIMO) wireless system [4]. The MIMO system also provides many features that are supposed to be present in 5G wireless communications, such as improving channel capacity and network performance without the need to add additional bandwidth (BW) or increase power at the source. The challenges facing MIMO system design are not limited to just enhancing the performance, but the compact size and low mutual coupling between individual antenna elements are also required for MIMO systems [5, 6].

The first challenge in MIMO design is the appropriate choice of antenna type which achieves high performance with small size. One of the most important types of antennas that is suitable to overcome this challenge and commonly used in 5G mobile phones is a modified folded dipole antenna. Since the conventional folded dipole antenna supports low and narrow BW, some modifications must be made to the conventional type of folded dipole antenna to increase its operating BW to be suitable for 5G NR applications. Cai and Sarabandi [7] introduced a modified compact size planar folded dipole antenna to obtain 53.2% broad BW and antenna gain of 1.6 dBi. One of the effective modifications that can be

Received 1 February 2022, Accepted 17 March 2022, Scheduled 1 April 2022

* Corresponding author: Alaa M. Hediya (alaahediya@gmail.com).

¹ Higher Institute of Engineering and Technology in Zagazig, Zagazig, Egypt. ² Microwave Engineering Department, Electronics Research Institute (ERI), Cairo, Egypt. ³ Electronics and Communications Engineering Department, Faculty of Engineering, Zagazig University, Zagazig, Egypt.

made to the folded dipole antenna to obtain multiple resonance frequencies is to divide the antenna into more than one part. In addition, a partial ground plane can be employed to extend the BW as well as improve the antenna's efficiency [8].

To overcome the second challenge, one of the separating methods is evolved to obtain a suitable degree of isolation among MIMO elements. The most common separating methods are using Defective Ground Surface (DGS), Frequency Selective Surface (FSS) structure, or Electromagnetic Band Gap (EBG) structure. EBG structure is a synthetic periodic crystal structure that stops wave propagation at certain frequency bands for all polarization types and all incident angles. Therefore, EBG structure can be used for improving the isolation between the antennas of a MIMO system in the corresponding frequency bandgap. This property improves the overall performance of the MIMO system and maintains the desired BW [3, 9]. The bandgap of an EBG structure can be calculated by using its dispersion diagram. Tu et al. [10] improved the mutual coupling and gain of a 4-element MIMO system by adding a round shape Double Side EBG (DS-EBG) structure. The use of an EBG substrate reduces the interaction between the antenna and human tissue. So, Specific Absorption Ratio (SAR) may also be reduced by employing this technique [9, 11].

In this research, a new design of an EBG structure is presented. This design introduces a frequency bandgap from 2.5 GHz to 6.5 GHz. The dispersion diagrams of the discussed EBG structures are calculated by using the Eigenmode Solver of CST Microwave Studio software. These EBG cells are added between the folded dipole antennas, which constitute the proposed 6-element MIMO antenna array. The aim of using EBG is to enhance the return loss of the elements of the array and increase the isolation between them, as well. Thus, the overall MIMO system parameters are improved. Another advantage of this design is that the SAR value of the MIMO system is significantly reduced. All designs and calculations of this paper were made by using CST Microwave Studio software.

The organization of this paper will be illustrated in the following sections. Section 2 presents the analysis and design of the EBG structure indicating the effect of the EBG structure on the antenna elements. Section 3 presents the analysis and design of the MIMO antenna array loaded by the designed EBG unit cells. The main properties of the MIMO system are discussed. In addition, the SAR analysis of this EBG-Loaded MIMO antenna array is also discussed. Section 4 provides the experimental results for the fabricated MIMO antenna array. The conclusion is presented in Section 5.

2. EBG STRUCTURE

A) Design of the EBG Unit Cell: The purpose of the EBG is to reduce the cross coupling between the elements constructing the MIMO system. The proposed antenna elements operate within the frequency BW from 3 to 5 GHz. The unit cell of the proposed EBG structure consists of a square spiral on each side of the substrate as shown in Fig. 1. The use of spiral shapes is appropriate to achieve the required high selective bandgap with a smaller EBG unit size and low insertion loss [12]. Vias between the spirals on both sides can also be used to control the stop and passbands as well as the width of the

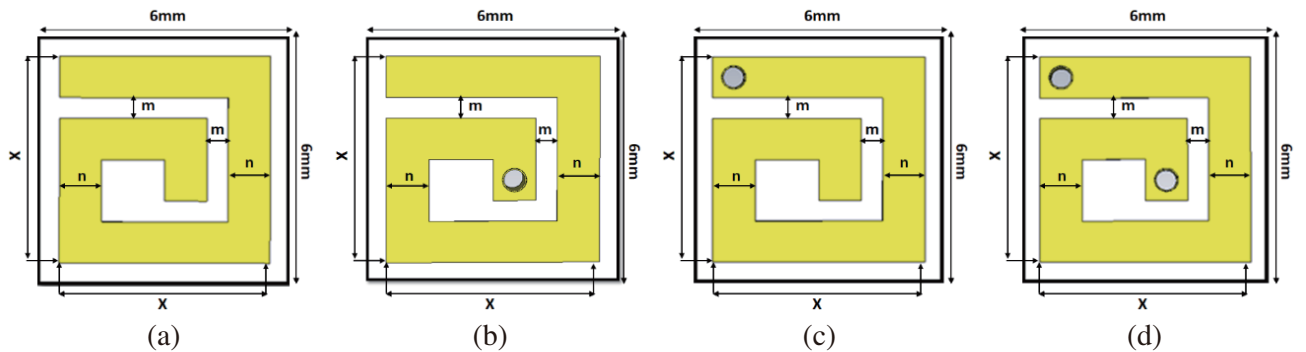


Figure 1. Different configurations for the unit cell of EBG structure, (a) without via, (b) with one middle via, (c) with one side via, (d) with two vias. Where the final dimensions of the proposed unit cell for the EBG structure, $X = 5$ mm, $n = 1$ mm, $m = 0.5$ mm, the diameter of the via = 0.5 mm.

bandgap. This spiral structure is printed on an FR4 substrate with ϵ_r equal to 4.3 and a thickness of 0.8 mm.

Several designs are studied for the EBG element as shown in Fig. 1 to study the effects of the via on the dispersion diagram. The first design is assumed to be without via. The second design has a via at the center of the spiral cell. The third design has a via at the free end of the spiral. Finally, the fourth design has two vias, at the center and the end of the spiral.

The dispersion diagrams are calculated for the four designs to determine the bandgap for each design as shown in Fig. 2 to determine the appropriate EBG design for the MIMO system. It is clear that the corresponding first bandgaps for the four designs are 4 : 8.5 GHz, 2.5 : 6.5 GHz, 2.2 : 6.2 GHz, and 5 : 8.6 GHz, respectively. Thus, the second and third designs have bandgaps that are suitable for the MIMO antenna operating from 3 to 5 GHz.

On the other hand, the effects of the different parameters of this unit cell are investigated on the second design specifically. Fig. 3 indicates the effect of varying the length of the unit cell (X). It is obvious that increasing X reduces the lower and upper edges of the bandgap. It also decreases the bandgap. The resulting bandgap, in this case, is from 1.6 to 4.8 GHz. On the other hand, decreasing X increases both the upper and lower limits of the bandgap while the bandgap is nearly removed.

The second parameter to be investigated is the spacing distance between the arms of the spiral (m). Fig. 4 indicates the effect of varying the value of m on the dispersion diagram. It can be noted that reducing the value of m reduces both the lower and upper edges of the bandgap as well as the value of the bandgap. On the other hand, increasing the value of m increases the lower edge of the bandgap

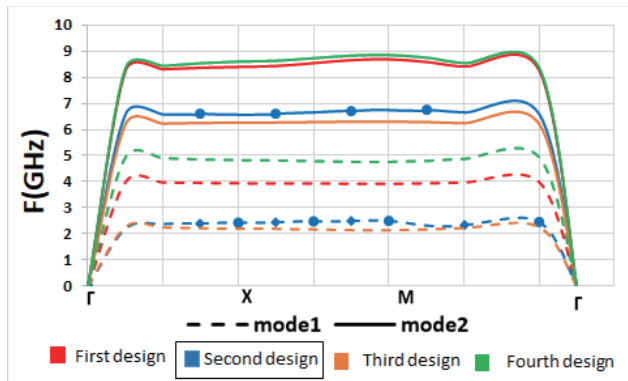


Figure 2. The dispersion diagram for different designs of EBG unit cell, depending on the number and location of the via.

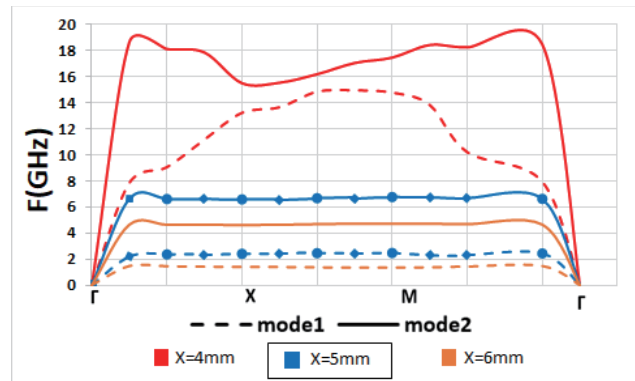


Figure 3. The effect of dimension X on the dispersion diagram for the second design in Fig. 1.

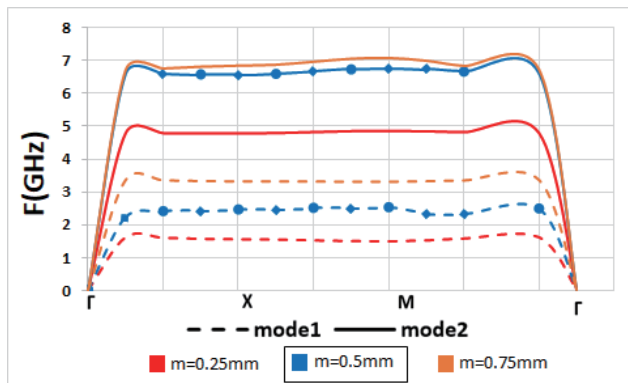


Figure 4. The effect of the dimension m on the dispersion diagram for the second design in Fig. 1.

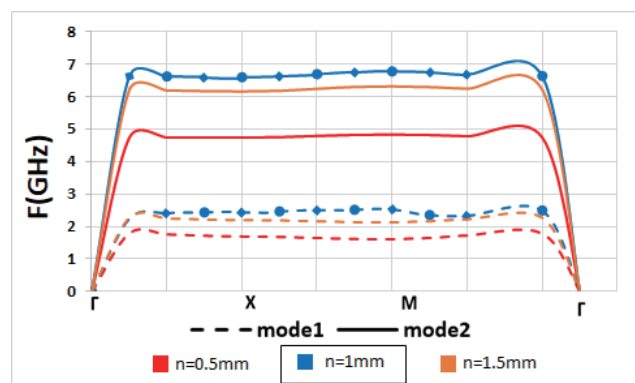


Figure 5. The effect of the dimension n on the dispersion diagram for the second design in Fig. 1.

such that in the case of $m = 0.75$ mm the lower edge of the bandgap exceeds the required frequency of 3 GHz.

Finally, Fig. 5 presents the effect of varying the width of the arm (n). It can be noted that increasing n introduces slight reductions in the upper and lower edges of the bandgap. However, reducing n introduces significant reductions in the lower and upper edges of the bandgap.

B) EBG Loaded Folded Antenna Element: The designed EBG unit cells are added adjacent to a folded dipole antenna to study its effect on the performance of the proposed antenna. The proposed folded dipole antenna is introduced in Fig. 6 with the details of its dimensions. The antenna's size is $(25 \times 12 \times 0.8)$ mm³. It was previously designed in [13] and loaded with a DGS substrate to improve the performance and other antenna parameters. In this research, the DGS has been replaced with EBG to obtain the best possible results for the antenna. The substrate parameters of this antenna element are the same as those of the EBG structure. The choice of the substrate material is an important factor in the design of the proposed antenna. FR-4 is considered a popular material suitable for different electrical applications and the fabrication of cell phones, because it has good electrical isolation, suitable fabrication characteristics, high efficiency, and low permittivity. It is also safe, easy to manufacture, and suitable for wideband applications [14, 15]. The antenna is placed at the edge of a mobile board of a standard size $(75 \times 134 \times 0.8)$ mm³ as shown in Fig. 7(a). This antenna has a partial ground plane with a distance L_g from the edge of the substrate as indicated in Fig. 7(b). Different values for L_g are investigated. It is found that the optimum value for L_g which introduces the minimum reflection coefficient and the best efficiency is 14 mm. The reflection coefficient and efficiency are presented in Fig. 8 and Fig. 9, respectively.

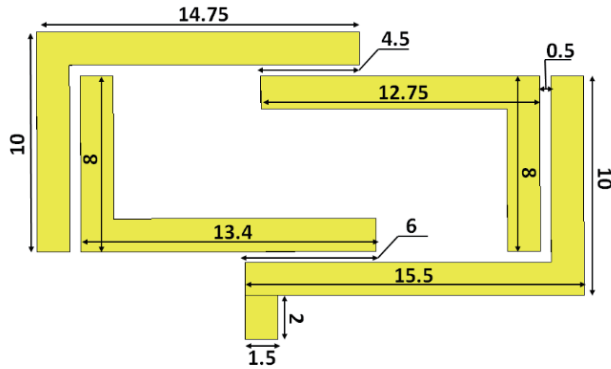


Figure 6. The detailed geometry in mm for the proposed folded dipole antenna.

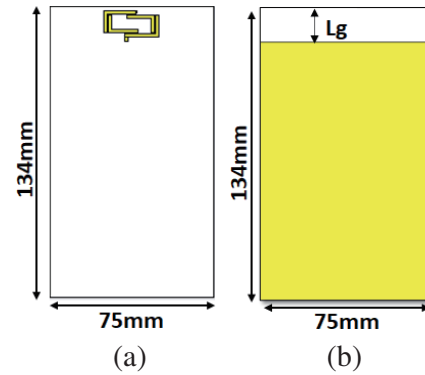


Figure 7. The Complete geometry of the folded dipole on a cell phone substrate. (a) Front view. (b) Back view.

It is obvious that the return-loss, in this case, is less than -8 dB in the desired frequency band, and the overall efficiency is 86% at a resonant frequency of 3.2 GHz. The radiation patterns and antenna gains of the individual antennas with a partial ground plane are calculated at the resonant frequency of 3.2 GHz and the two ends of the required frequency band as shown in Fig. 10. It is obvious that the maximum gain of the antenna in this configuration is about 1.5 dBi.

The effect of adding EBG unit cells on both sides of this folded antenna is studied for the two cases presented in Fig. 11. The results of the return-loss of the folded dipole antenna for these two cases and for the antenna with the partial ground plane where $L_g = 14$ mm are presented in Fig. 12. It is obvious that the existence of the EBG unit cell around the antenna element improves the corresponding return-loss compared with the use of a partially grounded plane only. It also improves the antenna efficiency as shown in Fig. 9. In addition, increasing the number of EBG unit cells introduces more improvement as shown in the comparison between the results of the first case and the second case of Fig. 12. The ideal case of EBG for the best performance is an infinity structure [16]. The antenna with 4×2 EBG array configuration achieved a return loss factor less than -12 dB over the BW of the antenna from 3 to 5 GHz. This structure also has three resonant frequencies at 3.2 GHz, 4.3 GHz, and 4.48 GHz.

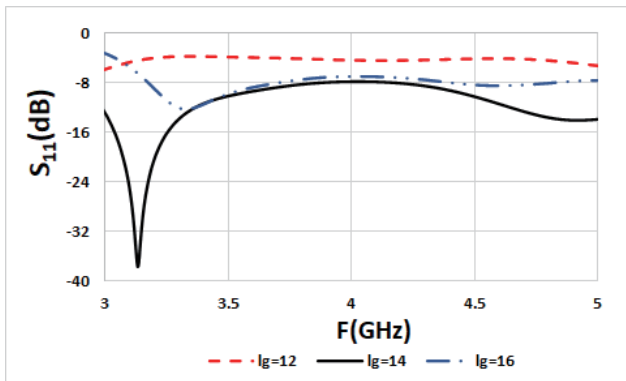


Figure 8. The simulated return loss of the designed folded dipole antenna with a partial ground plane at different values of L_g .

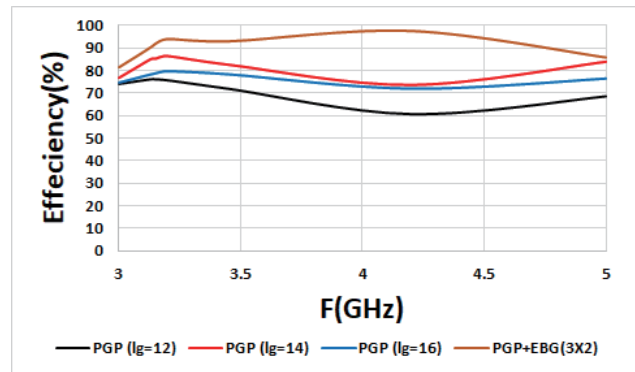


Figure 9. The simulated efficiency of the different configurations of designed folded dipole antenna.

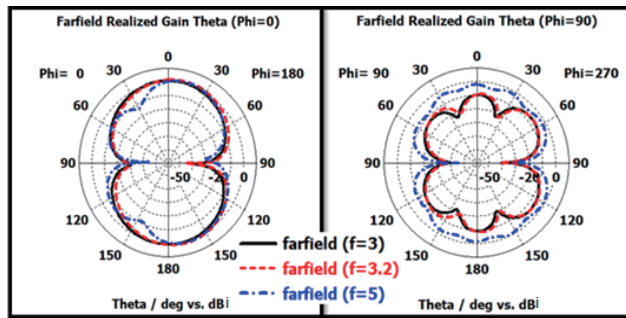


Figure 10. The gain of the proposed folded dipole antenna with a partial ground plane at different frequencies.

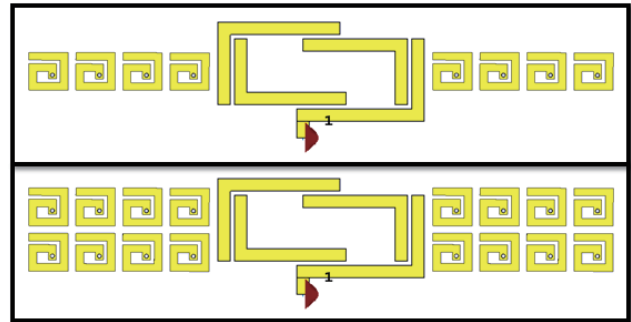


Figure 11. The different configurations of EBG structure constructed by changing the no of rows.

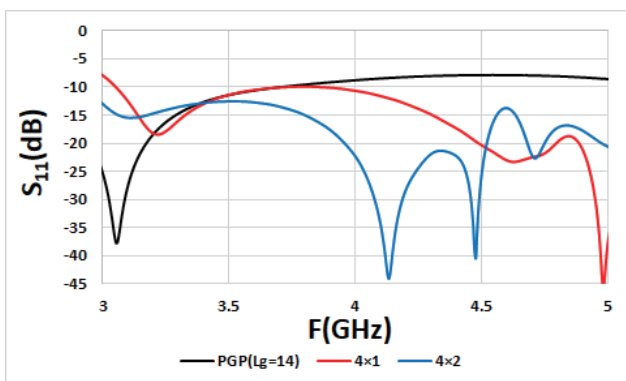


Figure 12. The simulated return loss of the proposed folded dipole antenna with 14mm partial ground plane and with different configurations of EBG structure constructed by changing the no of rows.

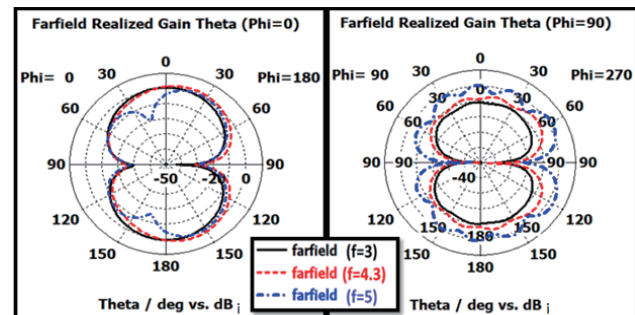


Figure 13. The gain of the proposed folded dipole antenna with a partial ground plane loaded with EBG at different frequencies.

The maximum efficiency of 97.3% is achieved at a resonant frequency of 4.3 GHz as indicated in Fig. 9. Thus, the second case was chosen as the final proposed antenna configuration. Fig. 13 introduces the radiation pattern and antenna gain at the resonance frequency of 4.3 GHz and the two boundaries of the BW for the proposed DS-EBG antenna configuration. It is clear that the maximum gain of 2.73 dBi is achieved at the resonant frequency of the antenna.

3. MIMO ANTENNA SYSTEM

A) MIMO Antenna Design: After achieving acceptable results for the single antenna element by employing partial ground plane and partial ground plane loaded with EBG structure, six elements of the same configurations are combined to form two configurations of the MIMO antenna system as presented in Fig. 14. The MIMO antenna system using a partial ground plane without EBG structure is presented in Figs. 14(a) and (b). The proposed MIMO antenna system with EBG unit cells is indicated in Figs. 14(c) and (d).

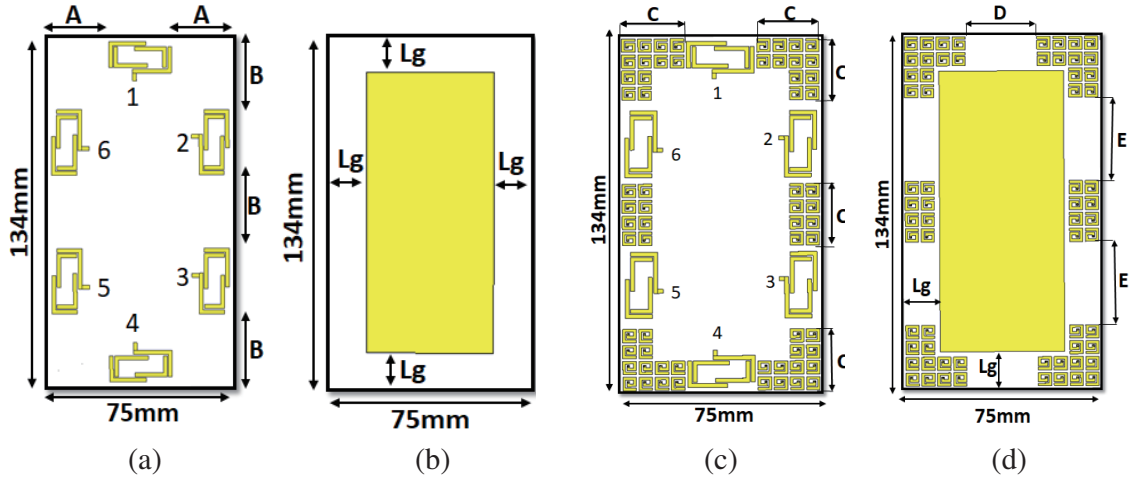


Figure 14. The geometry of the proposed MIMO antenna system of 6-elements on a cell phone substrate. (a) Front view without EBG, (b) Back view without EBG, (c) Front view with EBG, (d) Back view with EBG. ($A = 25$ mm, $B = 28$ mm, $C = 23$ mm, $D = 27$ mm, $E = 31.5$ mm and $L_g = 14$ mm).

A return loss of less than -6 dB is obtained for the proposed single antenna configuration which is considered as the maximum permissible limit for antennas in 5G application. However, this does not necessarily mean that it can be used in the MIMO system, because the return-loss coefficient for each antenna in the MIMO system may be affected by changing the location of the antenna inside the system and the induced mutual coupling with the other elements of the system. Thus, some antennas within the MIMO systems may achieve a return-loss factor greater than the maximum permissible limit of -6 dB.

The return loss coefficients of the six antennas within the partial ground plane MIMO system configuration were calculated as shown in Fig. 15. It is clear that some antennas of this MIMO system did not achieve an acceptable return loss coefficient. Fig. 16 shows that some antennas of the MIMO system did not achieve good values of mutual coupling coefficients, as well. Fig. 16 presents the isolation of the first antenna as an example of antennas isolation within this system. So, this system will not be suitable for 5G communications.

The simulated return loss for the six antennas of the EBG-MIMO system configuration is indicated in Fig. 17. It is obvious that all elements of this MIMO system have return-loss less than -9 dB over the desired BW. So, the EBG-MIMO system can be employed for the 5G communications.

For the proposed EBG-MIMO system, the mutual coupling between its elements achieved a value less than -20 dB. The mutual coupling coefficients between the first antenna and the other five elements

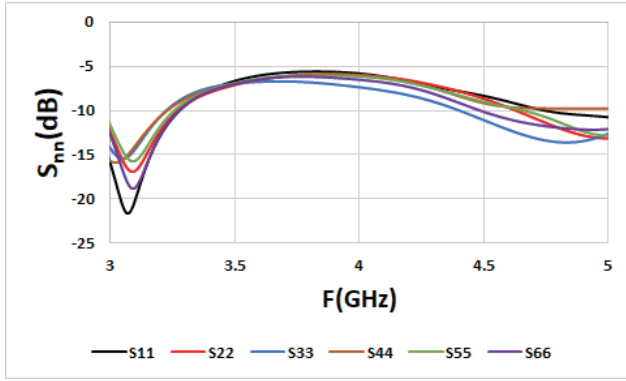


Figure 15. The return loss of the six antennas constituent partial ground plane MIMO system.

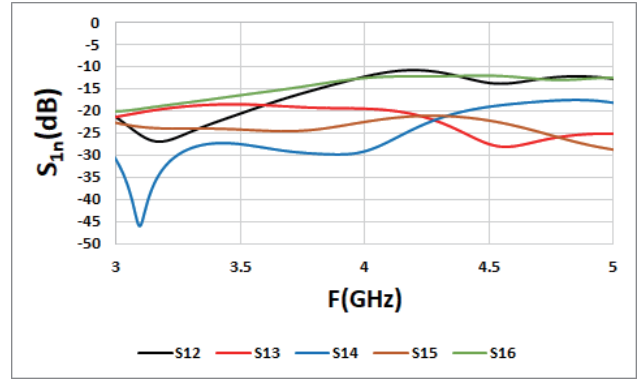


Figure 16. The simulated mutual coupling between Antenna 1 and other elements constituent partial ground plane MIMO system.

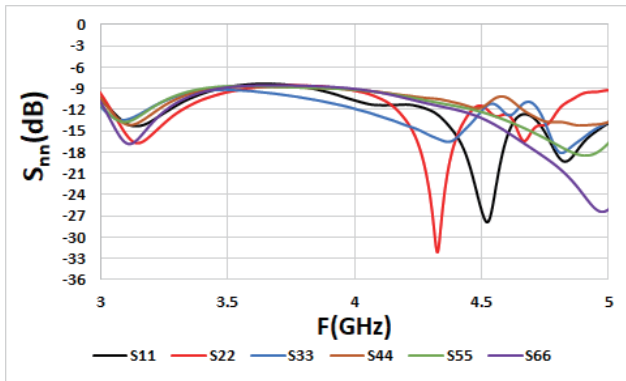


Figure 17. The return loss of the six antennas of the EBG-MIMO system.

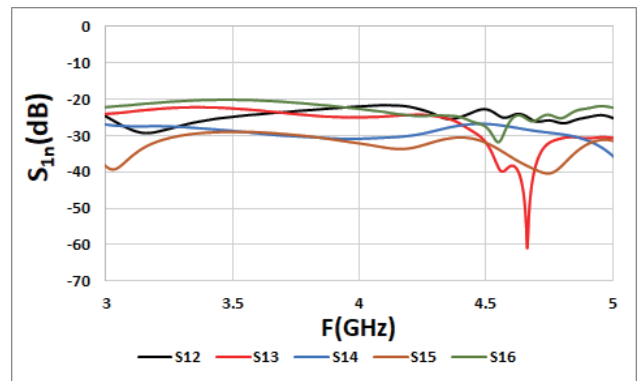


Figure 18. The simulated mutual coupling between Antenna 1 and other elements of the EBG-MIMO system.

are presented in Fig. 18 as an example of the coupling coefficients for the MIMO system. The results of Fig. 18 are enough to indicate the mutual coupling between the other antennas of the system because the results have some similarities with a slight difference due to the difference in the antenna location as well as the difference in the location of the feeding point of each antenna.

B) MIMO Antenna Parameters: The S -parameters of the MIMO system are necessary to calculate the related parameters of the proposed EBG-MIMO system, which distinguish the overall performance of the system. Several MIMO parameters like Envelop Correlation Coefficient (ECC), Diversity Gain (DG), Total Active Reflection Coefficient (TARC), Chanel Capacity Loss (CCL), and Mean Effective Gain (MEG) are calculated analytically to give a clear idea about the performance of the MIMO system.

ECC is considered as one of the most important parameters affecting the MIMO antenna system. Equation (1) presents the relation used to calculate the ECC [14]:

$$ECC_{m,n} = \frac{|S_{mm}^* S_{mn} + S_{nm}^* S_{nn}|^2}{(1 - |S_{mm}|^2 - |S_{mn}|^2)(1 - |S_{nm}|^2 - |S_{nn}|^2)^*} \quad (1)$$

The ECC frequency curve between the first antenna and other antennas of the proposed MIMO system is presented in Fig. 19 as an example of the ECC of the system elements. The values of ECC for all antennas are found to be less than 0.005, which falls within the suitable range of the MIMO systems for 5G applications. These results are acceptable for working as a high-performance MIMO antenna

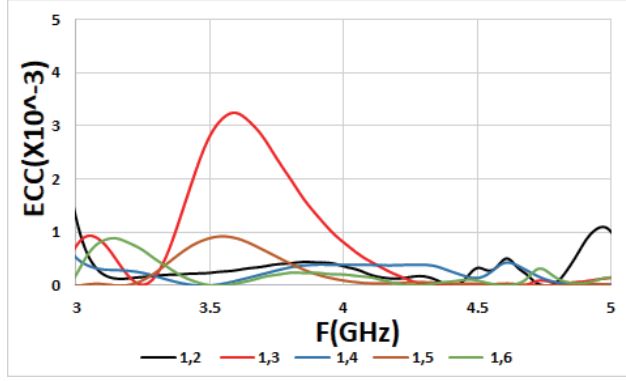


Figure 19. The ECC between Antenna 1 and other EBG-MIMO system antennas.

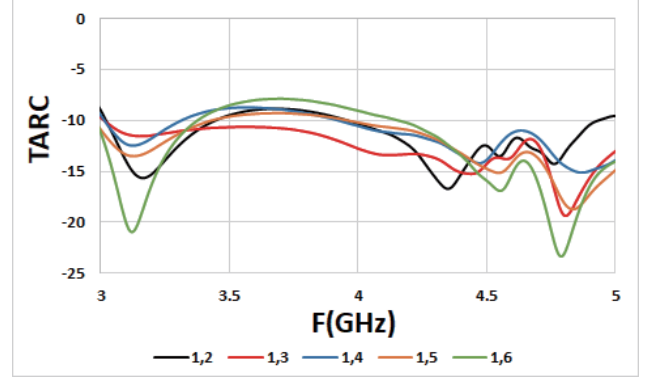


Figure 20. The TARC between Antenna 1 and other EBG-MIMO system antennas.

system, where the ECC parameter is required to be smaller than 0.5 [17].

The DG for the MIMO system indicates the losses in power transmitted when diversity charts are applied to the module. DG of 10 dB is obtained here, which is the amount required for MIMO antenna systems to ensure high performance [18]. DG is calculated according to the following equation [18]:

$$DG = 10\sqrt{1 - |ECC|^2} \quad (2)$$

TARC represents the apparent value of return loss of the antenna for the MIMO system. For 5G applications, the TARC value should be less than -6 dB [19]. The values of TARC for elements of the proposed MIMO system are found to be smaller than -8 dB. Fig. 20 shows the TARC curves versus frequency for the first antenna as an example of the TARC coefficients of other antennas within the proposed system. It is calculated using the following equation [14]:

$$TARC_{m,n} = -\sqrt{\frac{(S_{mm} + S_{nn})^2 + (S_{nm} + S_{mn})^2}{2}} \quad (3)$$

Another important MIMO system performance parameter is the CCL. The proposed MIMO antenna system has a CCL of 0.45 bit/s/Hz for the entire BW of the system, which is less than the practical standard [18]. Fig. 21 shows the first antenna CCL curves versus frequency as an example of CCL coefficients of the system elements. The CCL values are calculated according to the following

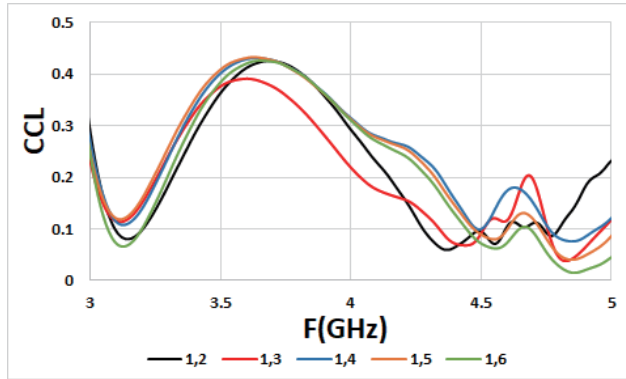


Figure 21. The CCL between Antenna 1 and other EBG-MIMO system antennas.

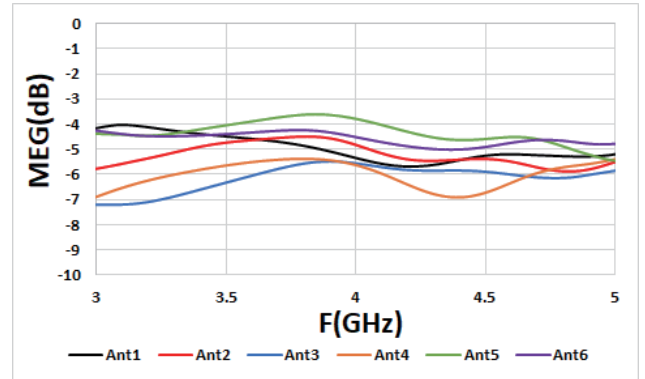


Figure 22. The MEG of the six elements of the EBG-MIMO system.

equations [18]:

$$ccl = -\log_2 \left(\left| \frac{\sigma_{m,m} \sigma_{m,n}}{\sigma_{n,m} \sigma_{n,n}} \right| \right) \tag{4}$$

where:

$$\sigma_{i,i} = 1 - \left(|S_{i,i}|^2 - |S_{i,j}|^2 \right) \tag{4a}$$

$$\sigma_{i,j} = - \left(S_{i,i}^* S_{i,j} + S_{j,i} S_{j,j}^* \right) \tag{4b}$$

The MEG parameter is also an effective diversity performance parameter for the analysis of MIMO systems. It is defined as the mean power received in the radiating environment. For highly diverse performance, the MEG value should be in the standard range from -3 dB to -12 dB for all elements of the MIMO system [20]. Fig. 22 presents the MEG for all elements of the proposed MIMO system. It is clear that the calculated MEG for the entire system is ranging from -7 dB to -10 dB which satisfies the required condition. The MEG is calculated according to the following relation [20]:

$$MEG_i = 05 \mu_{irad} = 05 \left(1 - \sum_{j=1}^k |S_{i,j}| \right) \tag{4c}$$

C) Hand Effect: For the design of the MIMO system to be complete, the effect of the human hand should be taken into consideration in the analysis of the overall performance of the system. Fig. 23 presents the comparison between the return loss coefficients for the six antennas of the MIMO system with and without the human hand model. It is obvious that the return losses are increased slightly due to the effect of the hand. However, the return losses for the six antenna elements with the presence of the human hand model are still within the limit of less than -6 dB.

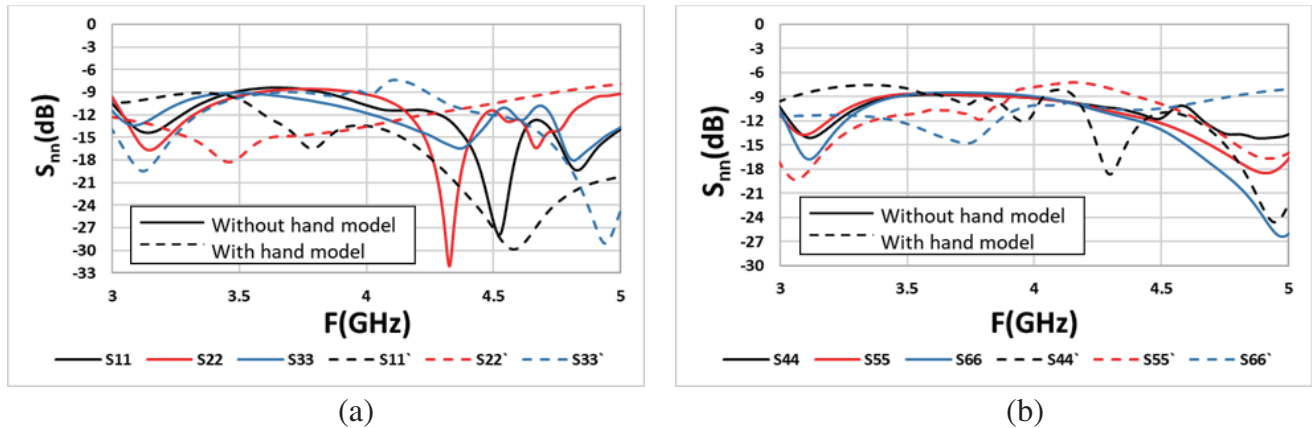


Figure 23. The return-losses for the six elements of the EBG-MIMO system with and without the hand model.

4. SAR CALCULATION

The SAR analyses of the proposed EBG-MIMO system are performed at 3.2 GHz and 4.2 GHz, which is one of the resonant frequencies of the antenna element with EBG. Calculations are made over 1 g tissue by inserting the MIMO system between the hand and head models of the CST simulator.

The proposed EBG-MIMO system achieved total SAR values of 0.5207615 W/Kg at the frequency of 3.2 GHz and 0.5890298 W/Kg at the frequency of 4.2 GHz. The total SAR of the proposed MIMO system is less than 0.6 W/Kg, which is much less than the international permissible value of 2 W/Kg.

5. EXPERIMENTAL RESULTS

The proposed MIMO system loaded with the EBG structure is fabricated and measured for verification. The fabricated antenna is presented in Fig. 24. The return loss coefficients for the six antennas of the fabricated MIMO system are indicated in Fig. 25. The value of the return loss coefficients increased over -10 dB, and the resonance frequency of some antennas changed. However, there is slight difference between the measured and simulated results of the return losses, and the results are still considered acceptable as they do not affect the overall performance of the MIMO system. The measured coupling coefficients between MIMO elements are presented in Fig. 26. It can be obvious that the measured and simulated coupling coefficients are very close. The measured coupling coefficients between all antennas are less than -20 dB.

Finally, two detailed comparisons between the proposed MIMO system and recently published MIMO systems are introduced in Table 1 and Table 2.

The comparison in Table 1 is related to the most important parameters required for the design of any antenna employed in MIMO systems. The comparison in Table 2 is based on the most important characteristics that affect the performance of the MIMO systems.

In Table 1, the reflection coefficient is calculated over the whole BW. The number of antenna elements within MIMO system is represented by N . The total size refers to the overall size of MIMO system. The SAR value represents the peak SAR value over the entire BW including resonant frequencies.

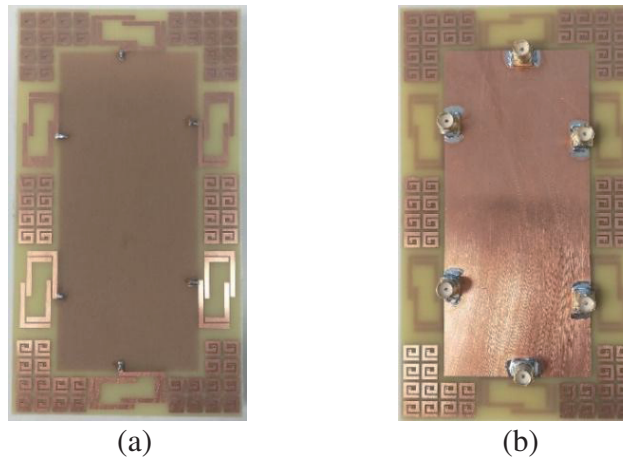


Figure 24. The front view (a) and the Back view (b) of the fabricated MIMO system.

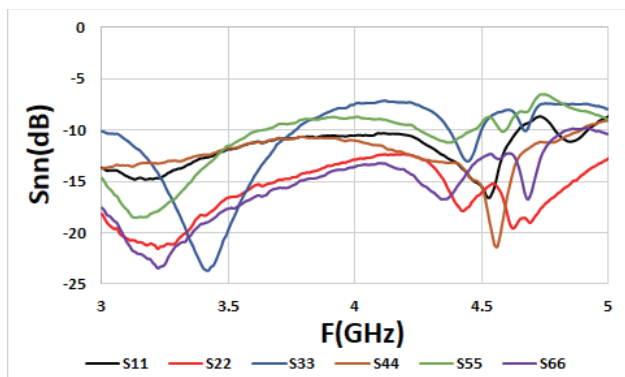


Figure 25. The measured return losses of the six antennas of the fabricated EBG-MIMO system.

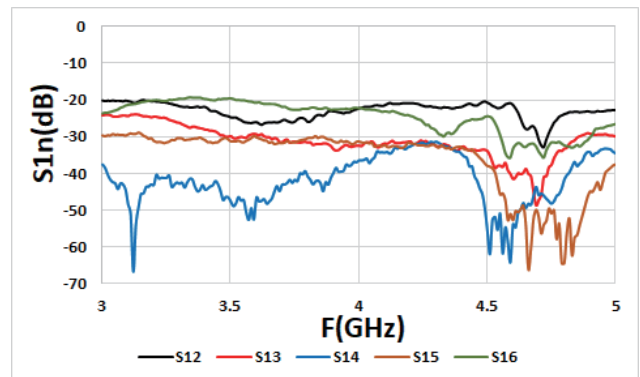


Figure 26. The measured mutual coupling between Antenna 1 and other elements of the fabricated EBG-MIMO system.

Table 1. A detailed comparison between the proposed MIMO system and the recently published work in terms of antenna parameters.

Reference	Type	BW	Reflection coefficient	N	Isolation method	Mutual coupling	Total size	SAR value	Application
[14]	Petal shaped slot antenna	(2550–2650) MHz	< –10 dB	8	NA	< –10 dB	(75 × 150 × 0.8) mm ³	NA	LTE cellular communication smartphone
[19]	Folded monopole antenna	(3300–3600) MHz	< –6 dB	8	Grounding branch	< –15 dB	(124 × 74 × 4) mm ³	< 1 W/Kg	5G smartphone applications
[21]	monopole antenna	(3.8–7.8) GHz	< –10 dB	2	mushroom -shaped EBG structure	< –15 dB	(31 × 20 × 1.6) mm ³	NA	compact wideband wireless devices
[22]	Microstrip planner square	Resonant at 5.8 narrow BW	–45 dB only at the resonant frequency	2	UC-EBG structure	Enhanced using EBG	(6.8 × 6.8 × 1.6) mm ³	NA	WLAN applications
[23]	Tailored antenna	(8–12) GHz	< –10 dB	2	EBG	< –22 dB	(55 × 49 × 1.6) mm ³	NA	X-band application
[24]	F-shaped antenna	(3.1–10.7) GHz	< –6 dB	4	Spiral EBG	< –15 dB	(23 × 23 × 19) mm ³	NA	UWB applications
[25]	flexible transparent antenna	(4.67–4.94) GHz	< –10 dB	2	NA	< –15 dB	(50 × 35 × 1.48) mm ³	NA	Sub 6 GHz and WLAN applications
[26]	flexible transparent antenna	(2.21–6) GHz	< –10 dB	4	NA	< –15 dB	(66 × 45 × 0.625) mm ³	NA	Sub 6 GHz applications
[13]	Coupled folded antenna	(3–5) GHz	< –7 dB	6	DGS	< –15 dB	(134 × 75 × 0.8) mm ³	< 2 W/Kg	N77, N78, and N79, 5G applications
Present work	Coupled folded antenna	(3–5) GHz	< –9 dB	6	DS-EBG	< –20 dB	(134 × 75 × 0.8) mm ³	< 0.6 W/Kg	N77, N78, and N79, 5G applications

From Table 1, comparing the proposed design with [19], [24], and [13] we find that the proposed MIMO system achieves good results in terms of return loss coefficient. As for the total SAR value, the proposed design achieved a better result than [19], while the rest of the references mentioned did not address the SAR value calculations. The proposed design is also better in terms of isolation than [14, 19, 21, 22, 24, 25, 26, 13]. As for [23], a high isolation value was achieved, but using only two individual elements.

Another comparison in terms of the characteristics affecting the performance of the MIMO system is described in detail in Table 2. By perusing this table, we can ensure that the overall performance of the proposed MIMO system gives promising results compared to the related work presented in the references.

Table 2. A detailed comparison between the proposed MIMO system and the recently published work in terms of MIMO characteristics.

Reference	ECC	DG = (10 dB)	TARC (dB)	CCL (bit/sec/Hz)	MEG (dB)
[14]	< 0.005	NA	< -16	NA	NA
[19]	< 0.21	NA	< -6	< 0.32	NA
[21]	NA	NA	NA	NA	NA
[22]	< 0.01	NA	NA	< 0.1	NA
[23]	< 0.016	✓	< -35	< 0.3	-3 < MEG < -5
[24]	< 0.02	✓	NA	NA	NA
[25]	< 0.05	✓	NA	< 0.5	Around 1
[26]	< 0.016	NA	NA	NA	NA
[13]	< 0.006	✓	< -7dB	< 0.6	-3 < MEG < -8
Present work	< 0.0045	✓	< -8	< 0.45	-7 < MEG < -10

6. CONCLUSION

In this research, a new design of square spiral EBG is used to enhance the overall performance of a proposed MIMO system consisting of six antenna elements. The role of the EBG in this design is to improve the return loss of the antenna and reduce the coupling between the elements of the proposed MIMO system with six radiators. Each element in the proposed MIMO system consists of a folded dipole antenna with four coupled sections. The proposed MIMO antenna system consists of six identical folded dipole elements operated at a BW from 3 to 5 GHz, which makes it suitable for N77, N78, and N79 NR bands. The simulation results indicate a good return loss coefficient less than -9 dB, high isolation over 20 dB, broad BW, and low SAR value under 0.6 W/Kg for the overall components of the system. Also, very good performance is obtained for the entire MIMO system compared to the recently published work, where the proposed work achieves ECC under 0.0045, DG around 10 dB TARC under -8 dB, CCL less than 0.45 bit/sec/Hz, and MEG from -7 dB to -10 dB. Finally, the proposed MIMO system is fabricated and measured to validate the simulation results. A good agreement is obtained between the simulated and measured results which indicates the validity and robustness of the proposed MIMO system.

REFERENCES

1. Sun, L., Y. Li, Z. Zhang, and Z. Feng, "Wideband 5G MIMO antenna with integrated orthogonal-mode dual-antenna pairs for metal-rimmed smartphones," *IEEE Transactions on Antennas and Propagation*, Vol. 68, 2494–2503, 2019.
2. Sim, C.-Y.-D., H.-Y. Liu, and C.-J. Huang, "Wideband MIMO antenna array design for future mobile devices operating in the 5G NR frequency bands n77/n78/n79 and LTE band 46," *IEEE Antennas and Wireless Propagation Letters*, Vol. 19, 74–78, 2020.
3. Dicandia, F. A. and S. Genovesi, "Exploitation of triangular lattice arrays for improved spectral efficiency in massive MIMO 5G systems," *IEEE Access*, Vol. 9, 17530–17543, 2021.
4. Desai, A., T. Upadhyaya, M. Palandoken, and C. Gocen, "Dual band transparent antenna for wireless MIMO system applications," *Microwave and Optical Technology Letters*, Vol. 61, 1845–1856, 2019.
5. Garg, P. and P. Jain, "Isolation improvement of MIMO antenna using a novel flower shaped metamaterial absorber at 5.5 GHz WiMAX band," *IEEE Transactions on Circuits and Systems II: Express Briefs*, Vol. 67, 675–679, 2019.
6. Khade, S. S. and S. Badjate, "Square shape MIMO antenna with defected ground structure," *2018 4th International Conference on Recent Advances in Information Technology (RAIT)*, 1–5, 2018.

7. Cai, X. and K. Sarabandi, "A compact broadband horizontally polarized omnidirectional antenna using planar folded dipole elements," *IEEE Transactions on Antennas and Propagation*, Vol. 64, 414–422, 2015.
8. Molins-Benlliure, J., M. Cabedo-Fabrés, E. Antonino-Daviu, and M. Ferrando-Bataller, "Effect of the ground plane in UHF Chip antenna efficiency," *2020 14th European Conference on Antennas and Propagation (EuCAP)*, 1–5, 2020.
9. Pikale, R., D. Sangani, P. Chaturvedi, A. Soni, and M. Munde, "A review: methods to lower specific absorption rate for mobile phones," *2018 International Conference On Advances in Communication and Computing Technology (ICACCT)*, 340–343, 2018.
10. Tu, D. T. T., N. T. B. Phuong, P. D. Son, and V. Van Yem, "Improving characteristics of 28/38 GHz MIMO antenna for 5G applications by using double-side EBG structure," *J. Commun.*, Vol. 14, 1–8, 2019.
11. El May, W., I. Sfar, J. M. Ribero, and L. Osman, "Design of low-profile and safe low SAR tri-band textile EBG-based antenna for IoT applications," *Progress In Electromagnetics Research Letters*, Vol. 98, 85–94, 2021.
12. Palandoken, M., *Metamaterial-based Compact Filter Design*, Intech Open, 2012.
13. Hediya, A. M., A. M. Attiya, and W. S. El-Deeb, "Multiple-input multiple-output antenna for sub-six GHz 5G applications using coupled folded antenna with defective ground surface," *Progress In Electromagnetics Research C*, Vol. 114, 13–29, 2021.
14. Parchin, N. O., H. J. Basherlou, Y. I. Al-Yasir, A. M. Abdulkhaleq, R. A. Abd-Alhameed, and P. S. Excell, "Eight-port MIMO antenna system for 2.6 GHz LTE cellular communications," *Progress In Electromagnetics Research C*, Vol. 99, 49–59, 2020.
15. Saleem, R., M. Bilal, H. T. Chattha, S. U. Rehman, A. Mushtaq, and M. F. Shafique, "An FSS based multiband MIMO system incorporating 3D antennas for WLAN/WiMAX/5G cellular and 5G Wi-Fi applications," *IEEE Access*, Vol. 7, 144732–144740, 2019.
16. Bhavarthe, P. P., S. S. Rathod, and K. Reddy, "A compact dual band gap electromagnetic band gap structure," *IEEE Transactions on Antennas and Propagation*, Vol. 67, 596–600, 2018.
17. Kulkarni, J., A. Desai, and C.-Y. D. Sim, "Wideband Four-Port MIMO antenna array with high isolation for future wireless systems," *AEU-International Journal of Electronics and Communications*, Vol. 128, 153507, 2021.
18. Khalid, M., S. Iffat Naqvi, N. Hussain, M. Rahman, S. S. Mirjavadi, M. J. Khan, et al., "4-Port MIMO antenna with defected ground structure for 5G millimeter wave applications," *Electronics*, Vol. 9, 71, 2020.
19. Jiang, W., Y. Cui, B. Liu, W. Hu, and Y. Xi, "A dual-band MIMO antenna with enhanced isolation for 5G smartphone applications," *IEEE Access*, Vol. 7, 112554–112563, 2019.
20. Rao, T., A. Sudhakar, and K. Raju, "Novel technique of MIMO antenna design for UWB applications using defective ground structures," 2018.
21. Kumar, J., "Compact MIMO antenna," *Microwave and Optical Technology Letters*, Vol. 58, 1294–1298, 2016.
22. Kumar, N. and U. K. Kommuri, "MIMO antenna H -plane isolation enhancement using UC-EBG structure and metal line strip for WLAN applications," *Radio Engineering*, Vol. 29, 2019.
23. Saxena, G., P. Jain, and Y. Awasthi, "High isolation EBG based MIMO antenna for X-band applications," *2019 6th International Conference on Signal Processing and Integrated Networks (SPIN)*, 97–100, 2019.
24. Modak, S. and T. Khan, "Cuboidal quad-port UWB-MIMO antenna with WLAN rejection using spiral EBG structures," *International Journal of Microwave and Wireless Technologies*, 1–8, 2021.
25. Desai, A., M. Palandoken, I. Elfergani, I. Akdag, C. Zebiri, J. Bastos, et al., "Transparent 2-element 5G MIMO antenna for sub-6 GHz applications," *Electronics*, Vol. 11, 251, 2022.
26. Desai, A., M. Palandoken, J. Kulkarni, G. Byun, and T. K. Nguyen, "Wideband flexible/transparent connected-ground MIMO antennas for sub-6 GHz 5G and WLAN applications," *IEEE Access*, Vol. 9, 147003–147015, 2021.